

Fluorescent derivatives of bile salts. III. Uptake of 7 β -NBD-NCT into isolated hepatocytes by the transport systems for cholytaurine¹

U. Schramm,* G. Fricker,† H-P. Buscher,** W. Gerok,** and G. Kurz^{2,*}

Institut für Organische Chemie und Biochemie der Universität Freiburg,* D-7800 Freiburg, Germany; Sandoz Pharma AG,† CH-4002 Basel, Switzerland; and Medizinische Universitätsklinik Freiburg,** D-7800 Freiburg, Germany

Abstract Uptake of 7 β -NBD-NCT ([N-[7-(4-nitrobenzo-2-oxa-1,3-diazol)]-7 β -amino-3 α ,12 α -dihydroxy-5 β -cholan-24-oyl]-2'-aminoethanesulfonate) in isolated rat liver hepatocytes occurs by saturable transport without being superimposed by simple diffusion. The dependency of flux rate of uptake on the concentration of 7 β -NBD-NCT in the presence of Na⁺ (143 mM) and with Na⁺ depletion (1 mM) is best described by the assumption of two simple transport systems. Maximal flux rates of uptake J_n and half-saturation constants K_T for 7 β -NBD-NCT are in presence of Na⁺ for transport system 1 $J_{1(Na^+143)} = 0.15 \pm 0.03$ nmol/(min · mg protein) and $K_{T1(Na^+143)} = 3.5 \pm 0.5$ μ M and for transport system 2 $J_{2(Na^+143)} = 1.0 \pm 0.1$ nmol/(min · mg protein) and $K_{T2(Na^+143)} = 190 \pm 25$ μ M, and in case of Na⁺ depletion $J_{1(Na^+1)} = 0.1 \pm 0.03$ nmol/(min · mg protein), $K_{T1(Na^+1)} = 3.0 \pm 0.5$ μ M, and $J_{2(Na^+1)} = 0.85 \pm 0.9$ nmol/(min · mg protein) and $K_{T2(Na^+1)} = 195 \pm 27$ μ M. Uptake of 7 β -NBD-NCT by both transport systems is competitively inhibited by cholytaurine in the presence of Na⁺ and with Na⁺ depletion. Two transport systems are likewise involved in the uptake of cholytaurine in the presence of Na⁺ as well as in case of Na⁺ depletion. Their kinetic parameters are in presence of Na⁺ $J'_{1(Na^+143)} = 1.55 \pm 0.14$ nmol/(min · mg protein) and $K'_{T1(Na^+143)} = 16.1 \pm 3.0$ μ M, and $J'_{2(Na^+143)} = 0.51 \pm 0.05$ nmol/(min · mg protein) and $K'_{T2(Na^+143)} = 38.0 \pm 4.1$ μ M, and in case of Na⁺ depletion $J'_{1(Na^+1)} = 0.10 \pm 0.02$ nmol/(min · mg protein), $K'_{T1(Na^+1)} = 7.7 \pm 1.2$ μ M, and $J'_{2(Na^+1)} = 0.40 \pm 0.03$ nmol/(min · mg protein) and $K'_{T2(Na^+1)} = 41.0 \pm 4.2$ μ M. Uptake of cholytaurine by both transport systems is competitively inhibited by 7 β -NBD-NCT in the presence of Na⁺ as well as in case of Na⁺ depletion. In both cases the inhibition constants are practically identical with the K_T values for uptake of 7 β -NBD-NCT. Photoaffinity labeling of isolated hepatocytes using 7,7-ACT (400 μ M) resulted in the irreversible inhibition of uptake of both bile salts to similar extents, confirming the kinetic data that 7 β -NBD-NCT is a true analogue of cholytaurine. —Schramm, U., G. Fricker, H-P. Buscher, W. Gerok, and G. Kurz. Fluorescent derivatives of bile salts. III. Uptake of 7 β -NBD-NCT into isolated hepatocytes by the transport systems for cholytaurine. *J. Lipid Res.* 1993. 34: 741-757.

Supplementary key words bile salt secretion • hepatobiliary transport • competing substrates • fluorescence microscopy • Na⁺ dependency • photoaffinity labeling

The morphological complexity of the liver, the biochemical complexity of transcellular transport, and the physicochemical properties of bile salts make the study of hepatobiliary bile salt transport extremely laborious. Attachment of a fluorophor (fluorescent group) to a bile salt molecule allows investigators to overcome some of the difficulties and offers new possibilities for the study of transport at the organ level by visualizing bile salt transport with the aid of fluorescence microscopy (1-3). Used as a fluorophor, the NBD-amino group linked to the steroid structure by the amino function has two advantages, 1) the monoanionic character of the bile salt is not changed; and 2) different synthetic diastereomeric derivatives are easily accessible (4). However, the addition of even a small fluorophor, the optical properties of which presuppose an extended π -electron system, to a bile salt may lead to alterations in its physiological behavior. In order to be relevant for the study of bile salt transport by fluorescence microscopy, a fluorescent derivative must be a true analogue of the physiological molecule, and as such it has to meet a rigid set of criteria. In the biological system to be investigated, a fluorescent derivative must behave as an analogue of the physiological bile salt in terms of metabolism, transport, and toxicity. Thus, a fluorescent derivative must be qualitatively metabolized and transported by the same pathways and mechanisms as the

¹Dedicated to Professor Gustav Paumgartner on the occasion of his 60th birthday.

²To whom correspondence should be addressed.

Abbreviations: 7,7-ACT, (7,7-azo-3 α ,12 α -dihydroxy-5 β -cholan-24-oyl)-2'-aminoethanesulfonate; [³H]-7,7-ACT, (7,7-azo-3 α ,12 α -dihydroxy-5 β -cholan-24-oyl)-2'-[2'-³H(N)]aminoethanesulfonate; EGTA, ethylene glycol-bis(β -aminoethyl ether)-N,N,N',N'-tetraacetic acid; NBD, 4-nitrobenzo-2-oxa-1,3-diazol; 7 β -NBD-NCT, [N-[7-(4-nitrobenzo-2-oxa-1,3-diazol)]-7 β -amino-3 α ,12 α -dihydroxy-5 β -cholan-24-oyl]-2'-aminoethanesulfonate; [³H]-7 β -NBD-NCT, [N-[7-(4-nitrobenzo-2-oxa-1,3-diazol)]-7 β -amino-3 α ,12 α -dihydroxy-5 β -cholan-24-oyl]-2'-[2'-³H(N)]aminoethanesulfonate; SDS-PAGE, sodium dodecyl sulfate polyacrylamide gel electrophoresis.

physiological bile salt, and the tolerance of the biological system must be similar for both compounds. These criteria are fulfilled differently for different stereoisomeric taurine-conjugated fluorescent bile salt derivatives, depending on the position and orientation of the NBD-amino group (5).

7β -NBD-NCT is a fluorescent derivative that appears to satisfy the requirements as an analogue of cholytaurine in hepatic transport. It is not metabolized during hepatobiliary transport, it interacts intracellularly with the same proteins as cholytaurine, and it is secreted into bile by the pathway for bile salts (4, 5). Only with regard to the uptake of 7β -NBD-NCT into hepatocytes has the analogy with cholytaurine not been shown conclusively.

The uptake of a compound through the sinusoidal membrane into hepatocytes may occur by different transport systems and mechanisms, because liver as an organ of detoxication is involved in the elimination of numerous compounds with different structures and charges. The attachment of a fluorescent group to a physiological bile salt molecule may result in an alteration of hepatic uptake, depending on the specificity of sinusoidal transport processes. Uptake of the fluorescent bile salt derivative 7β -NBD-NCT may occur by transport processes that are either completely different from that for bile salts or partially different, if in addition to bile salt transport processes other uptake processes are involved, or by transport processes that are the same as for physiological bile salts.

In order to be suitable for the study of bile salt transport by fluorescence microscopy, 7β -NBD-NCT must be transported as a true competing substrate by the same, and only the same, processes as the physiological bile salt cholytaurine. Sinusoidal uptake of cholytaurine is generally assumed to occur by different processes, a saturable Na^+ -dependent transport, a saturable Na^+ -independent transport, and a nonsaturable transport independent of Na^+ . However, the kinetic analyses are open to serious objections. Therefore, in the present report, the uptake of 7β -NBD-NCT as well as that of cholytaurine were characterized kinetically and clear evidence is presented that both bile salts are taken up into isolated rat hepatocytes by the same two transport systems. This allows the application of 7β -NBD-NCT for the study of hepatobiliary bile salt transport by fluorescence microscopy.

MATERIALS AND METHODS

Materials

7β -NBD-NCT and [^3H] 7β -NBD-NCT (750–1500 GBq/mmol), cholyl[2'- ^3H (N)]taurine (750–1500 GBq/mmol), 7,7-ACT and [^3H]7,7-ACT (750–1500 GBq/mmol) were synthesized as described (4, 6). (Hydroxy[^{14}C]methyl)inulin

was purchased from Amersham Buchler (Braunschweig, Germany). Cholytaurine (Na^+ salt) was purchased from Sigma Chemie GmbH (Taufkirchen, Germany). Collagenase "Worthington" CLS II with a specific activity of 125–150 u/mg protein was obtained from Biochrom KG (Berlin, Germany). Silicone oils AR 20 and AR 200 were obtained from Wacker Chemie (München, Germany). Trypan blue was from Serva (Heidelberg, Germany). All other substances were purchased from the usual commercial sources at the highest purity available.

Animals

Male Wistar rats (Tierzuchtanstalt Jautz, Hannover, Germany) weighing 200–250 g were used. The animals had free access to food (standard rat diet Altromin 300 R, Altromin GmbH, Lage, Germany) and tap water and were housed in a constant temperature environment with natural day–night rhythm.

Rat ascites hepatoma AS-30 D was obtained from Dr. D. Keppler (Institut für Tumorbiochemie, Deutsches Krebsforschungszentrum, Heidelberg, Germany) and propagated into 7- to 9-week-old male Wistar rats at 7-day intervals by intraperitoneal injection.

Quantitative determinations

Protein was determined by a modified biuret method (7) using chloroform instead of ether to remove turbidity due to lipid. Bovine serum albumin was used as the standard. Activity of alanine aminotransferase (L-alanine:2-oxoglutarate aminotransferase EC 2.6.1.2), and of glutamine synthetase (L-glutamate:ammonia ligase (ADP-forming), EC 6.3.1.2) were determined as described (8, 9). ATP was determined enzymatically in neutralized supernatants from perchloric acid-treated cell samples (10).

Isolation of hepatocytes

Isolated hepatocytes from rat livers were prepared by a modified collagenase perfusion method using a two-step procedure (11–13). All procedures were carried out at 37°C. After exposure of the liver of pentobarbital-anesthetized rats (3 mg of sodium pentobarbital/100 g of body weight, i.p.) by abdominal incision, a 16-G cannula was placed in the portal vein and connected to a nonrecirculating buffer reservoir containing a Ca^{2+} -free buffer consisting of 118 mM NaCl, 4.74 mM KCl, 1.2 mM MgCl_2 , 0.59 mM KH_2PO_4 , 0.59 mM Na_2HPO_4 , 24 mM NaHCO_3 , and 5.5 mM D-glucose, saturated with carbogen (95% O_2 /5% CO_2) and adjusted to pH 7.4. Immediately after connection of the cannula with the buffer reservoir, the perfusion was started and the inferior vena cava was cut. The pressure during all perfusion steps was maintained at 12 cm \pm 0.5 cm water pressure. The liver was severed from its in situ connections and cautiously transferred to a liver dish in a liver perfusion apparatus. In order to lower Ca^{2+} concentration, after 5 min the per-

fusion was continued without recirculation for exactly 5 min using the same buffer containing, in addition, 450 μM EGTA. Subsequently the liver was flushed for 10 min with the Ca^{2+} -free buffer. Thereafter, the recirculating collagenase perfusion was performed with 100 ml of buffer containing 118 mM NaCl, 4.74 mM KCl, 1.2 mM MgCl_2 , 0.59 mM KH_2PO_4 , 0.59 mM Na_2HPO_4 , 24 mM NaHCO_3 , 1.25 mM CaCl_2 , and 5.5 mM D-glucose, which was saturated with carbogen (95% O_2 /5% CO_2) and adjusted to pH 7.4 (standard buffer), and additionally supplied with collagenase (about 7500 units) so that a perfusion time of 12–15 min for complete disintegration of the liver was not exceeded. The amount of collagenase needed proved to be dependent on the lot of enzyme. After 15 min of perfusion with collagenase, the liver was transferred into a crystallization dish containing 100 ml standard buffer. The capsule was disrupted and the isolated cells were liberated by shaking the liver first gently and then vigorously to liberate the inner cells. To remove cell aggregates and tissue fragments, the crude cell suspension was passed through a Thomapo nylon filter with a mesh size of 79 μm (Reichelt, Heidelberg, Germany). Intact hepatocytes were separated from nonparenchymal cells and cell debris by centrifugation at 35 g for 2 min. The supernatant was discarded, the sedimented cells were resuspended in 100 ml standard buffer, and the suspension was centrifuged a second time under the same conditions. The isolated hepatocytes ($3.8\text{--}4.0 \times 10^8$ cells) were finally resuspended in standard buffer to give a suspension of $2.5\text{--}3 \times 10^6$ cells/ml (5–6 mg protein/ml). The freshly isolated hepatocytes were allowed to recover by gently shaking the cell suspension at 37°C under an atmosphere of carbogen for 30–60 min.

For uptake studies in Na^+ -depleted medium, the sedimented hepatocytes obtained after separation of the nonparenchymal cells were suspended and washed three times with choline buffer containing 118 mM choline chloride, 4.74 mM KCl, 1.2 mM MgCl_2 , 0.59 mM KH_2PO_4 , 0.59 mM K_2HPO_4 , 24 mM choline hydrogen carbonate, 1.25 mM CaCl_2 , and 5.5 mM D-glucose, which was saturated with carbogen (95% O_2 /5% CO_2) and adjusted to pH 7.4 (Na^+ -depleted medium).

Experiments with freshly isolated hepatocytes were performed within 2–2.5 h after isolation.

Characterization of the freshly isolated hepatocytes

Cell viability was estimated immediately after isolation and at the end of the experiments by determining Trypan blue exclusion. Only cell suspensions of hepatocytes with a viability of >90% immediately after isolation were used. The viability of these cells did not decrease more than 3% during the time necessary for the experiments. In order to control the viability of the hepatocytes that were used, the ATP content of the recovered cells was determined (10). Uptakes obtained by hepatocyte suspen-

sions with an ATP content of <13.1 nmol/mg protein were not further analyzed. Thereby, only results with cell suspensions having an adequate ATP level were taken into account, as recently proposed for metabolic studies with isolated hepatocytes (14).

The presence of the small number of perivenous hepatocytes was controlled by estimation of the activity of glutamine synthetase, a unique enzymatic activity characteristic for these cells. The specific activity of glutamine synthetase was 300 mU/mg protein.

Photoaffinity labeling

Photoaffinity labeling of isolated hepatocytes that were used for uptake studies was performed with 10 ml of a hepatocyte suspension ($2.5\text{--}3 \times 10^6$ cells/ml; 5–6 mg protein/ml) in presence of 400 μM 7,7-ACT with and without preincubation for 5 min. Photolysis was carried out at 30°C as described (5). After photoaffinity labeling the hepatocytes were freed from residual 7,7-ACT and its photolysis products by centrifugation at 35 g for 2 min, and resuspended in 50 ml of standard buffer. After repeating this procedure four times, the hepatocytes were finally resuspended in 10 ml of standard buffer and the cell suspension was allowed to recover at 37°C for 30 min. Cell viability was determined by Trypan blue exclusion.

Photoaffinity labeling of isolated hepatocytes, performed in order to identify bile salt-binding polypeptides, was carried out with 0.5 ml of a hepatocyte suspension with 50 μM of [^3H]7,7-ACT at 30°C as described (5).

Photoaffinity labeling of membrane subfractions enriched with canalicular membranes and of liver snips with [^3H]7,7-ACT was performed as described (15, 16).

Discontinuous SDS-PAGE using vertical slab gels ($200 \times 180 \times 2.8$ mm) was performed as described (17).

Uptake studies

Uptake of 7β -NBD-NCT and of cholytaurine was determined using the centrifugal filtration technique through silicone oil layer (18, 19). All solutions were kept at a temperature of 37°C. Uptake of the bile salts was started by the addition of 600 μl of a suspension of hepatocytes in the appropriate buffer to 600 μl of standard buffer or of Na^+ -depleted medium containing the corresponding labeled bile salt (1 μM to 1 mM). Cholytaurine and 7β -NBD-NCT were applied as their Na^+ salts. In the Na^+ -depleted medium the low concentration of $1 \text{ mM} \pm 0.1 \text{ mM}$ Na^+ was adjusted with NaCl because it is almost impossible to work with isolated hepatocytes in an absolutely Na^+ -free medium. Each distinct concentration of the bile salt contained 37 kBq of its tritium-labeled derivative, so that the specific radioactivity of the labeled bile salt decreased with increasing concentrations, whereas the absolute radioactivity remained constant. For competition studies the competing bile salt was added unlabeled to standard buffer or Na^+ -depleted medium in the

appropriate concentrations. In all transport studies involving a competing substrate, uptake was determined in parallel without the competing substrate. In all studies determining the Na⁺-independent flux rates in Na⁺-depleted medium, the control measurements in Na⁺-containing standard buffer were always performed in parallel.

The incubation suspension was swirled and aliquots of 100 μl were removed at precisely fixed times and placed into a 0.5-ml centrifuge tube containing 10 μl 0.75 M HClO₄ and overlaid by a 150 μl silicone layer (AR20:AR200 = 1:1). During centrifugation in the Beckman Microfuge B (Beckman Instruments, München, Germany) the cells were separated from incubation medium through the silicone into the denaturation layer within 1–2 sec. Incubation medium adherent to the sedimented cells was estimated separately from the amount of (hydroxy[¹⁴C]methyl)inulin precipitated with the cells.

Initial rates of uptake were routinely obtained from 15 sec up to 120 sec in 15-sec intervals and were guaranteed over the complete concentration range by control measurements in the time period between 2 and 15 sec. For these measurements 50 μl of the preheated buffer containing the appropriate concentration of labeled bile salt placed above the silicone oil layer was mixed with 50 μl of hepatocyte suspension in the centrifuge tube. At different times after initiation uptake was stopped by starting the centrifugation.

Radioactivity was determined in the complete cell pellet fraction and, in a few cases, for control in the supernatant incubation medium using 20-μl aliquots. For determination of radioactivity in the cell pellet, the tubes were shock-frozen in liquid nitrogen and cut at the phase interface between the denaturation layer and the silicone oil layer.

Detection of radioactivity

Radioactivity was determined by liquid scintillation counting (RackBeta 1217, Pharmacia LKB, Freiburg, Germany). Four ml Quickszint 1 (Zinsser Analytic GmbH, Frankfurt, Germany) was added to aqueous solutions and 4 ml Quickszint 501 (Zinsser Analytic GmbH) was added to the denaturation layer after dissolving the cell pellet by incubation in 500 μl Biolute (Zinsser Analytic GmbH) for 12 h at 40°C. Detection of radioactivity in polyacrylamide gels was performed as described (20).

Data analyses

Initial rates of uptake of 7β-NBD-NCT and of cholyltaurine were determined from the slope in the linear range by linear regression analysis, generally considering only the first four measuring points.

Kinetic parameters were analyzed by the nonlinear least-squares regression analysis program ENZFITTER 1.05 (Elsevier-BIOSOFT, Cambridge, UK) in the J-against-A-

diagram taking all data points into account with the same weight. In general, uptake studies were performed 15 times and inhibition studies 5 times using a separate preparation of cells for each experiment, and each study was analyzed separately. The resulting kinetic data are reported as means ± SEM. Statistic differences were determined by Student's *t*-test.

Fluorescence microscopy

Isolated hepatocytes (1 × 10⁶ cells/ml) were incubated

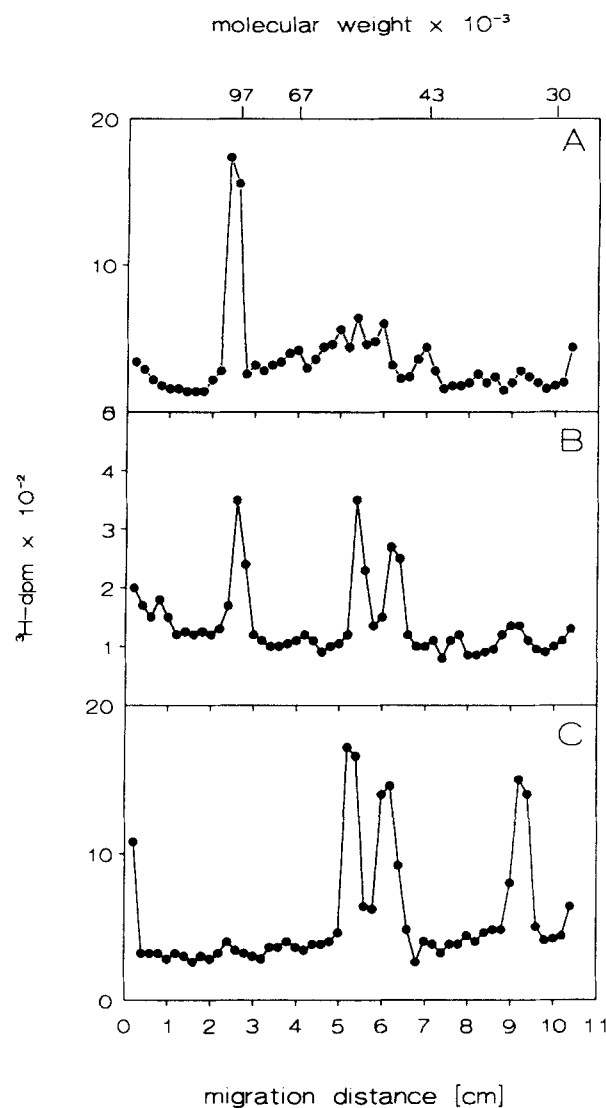


Fig. 1. Comparison of bile salt-binding membrane polypeptides, identified by photoaffinity labeling in canaliculi membrane subfraction (A), in intact liver tissue (B), and in freshly isolated hepatocytes (C). A: Membrane subfraction enriched with canaliculi membranes containing 0.5 mg of protein was photolabeled with 2.8 μM (370 kBq) [³H]7,7-ACT. B: Forty liver snips (1 × 1 × 2 mm³) were preincubated with 4 μM (15 mBq) [³H]7,7-ACT for 10 min in the dark at 37°C and subsequently photolabeled. C: Freshly isolated hepatocytes (2.5 × 10⁶) were preincubated with 20 μM (370 kBq) [³H]7,7-ACT for 5 min and subsequently photolabeled. SDS-PAGE was performed using a total acrylamide concentration of 10.5% at a ratio of acrylamide-bisacrylamide of 97.2:2.8.

with 1–50 μM $7\beta\text{-NBD-NCT}$ in standard buffer and directly examined by incident light fluorescence using a Polyvar fluorescent microscope (Reichert-Jung, Nussloch, Germany) equipped with an excitation filter 450–495 nm, dichroic mirror 510 nm, and barrier filter 520–560 nm. Photographs were recorded on Kodak Ektachrome 400 film.

RESULTS

Absence of bile salt secretion in freshly isolated hepatocytes

An integral membrane polypeptide with an apparent M_r of about 110,000 has been identified as being involved in canalicular bile salt secretion (15, 16, 21, 22), an ATP-dependent process (23, 24). In order to determine whether not only bile salt uptake but also a process corresponding to bile salt secretion in intact liver tissue is operative in freshly isolated hepatocytes, comparative photoaffinity labeling studies were performed, on the one hand with isolated bile canalicular membranes and intact liver tissue and, on the other hand, with freshly isolated hepatocytes. Relatively high concentrations of up to 50 μM of the photolabile bile salt derivative [^3H]7,7-ACT were used for the photoaffinity labeling experiments, and the complete particulate fractions of intact liver snips and of the freshly isolated hepatocytes were analyzed subsequent to photoaffinity labeling. Thus, the bile salt-binding polypeptide with the apparent M_r of about 110,000 could not elude chemical detection. Whereas both in membrane subfractions enriched with canalicular membranes (Fig. 1A) and in intact liver snips (Fig. 1B) the polypeptide with the apparent M_r of 110,000 was found to be clearly labeled, there was no indication that radioactivity was incorporated into this polypeptide using freshly isolated hepatocytes (Fig. 1C). When hepatocytes were loaded to 1 mM [^3H]ACT concentration internally and the efflux was studied, no incorporation of radioactivity into the polypeptide with the apparent M_r of 110,000 could be achieved. Because [^3H]ACT interacts intracellularly with different bile salt-binding polypeptides, its thermodynamically active concentration is not identical with its total intracellular concentration of 1 mM considering a cell volume of 3 $\mu\text{l}/\text{mg}$ protein. The lack of labeling of a polypeptide with the apparent M_r of about 110,000 in freshly isolated hepatocytes was not due to a decrease of the intracellular ATP-level, because an ATP-content of the freshly isolated hepatocytes >13.1 nmol/mg protein should be sufficient to guarantee bile salt secretion. In freshly isolated hepatocytes, canalicular bile salt secretion corresponding to the secretion process in liver does not occur and therefore it must be assumed that bile salt efflux from isolated hepatocytes occurs by reversal of the uptake process.

Heterogeneity of $7\beta\text{-NBD-NCT}$ uptake into freshly isolated hepatocytes

In order to estimate the suitability of the freshly isolated hepatocytes for the study of bile salt uptake and to compare the capability of single cells quantitatively for bile salt uptake, hepatocyte suspensions were incubated with 1–10 μM $7\beta\text{-NBD-NCT}$ and its uptake was visualized by fluorescence microscopy. The fluorescent derivative was readily taken up into the freshly isolated hepatocytes as demonstrated with 5 μM $7\beta\text{-NBD-NCT}$ after 45 sec (including the exposure time) by the fluorescence micrograph (Fig. 2A). The most interesting observation, the heterogeneity of fluorescence, was more evident after 2 min of incubation and separation from the incubation medium for lowering the fluorescent background (Fig. 2B). This heterogeneity of fluorescence, which could always be observed, showed no correlation with the size of the cells. It indicates that the velocity of uptake of $7\beta\text{-NBD-NCT}$ is different for different hepatocytes.

Absence of bile salt uptake by simple diffusion

In addition to mediated transport, uptake by simple diffusion has been taken into consideration for bile salt transport into hepatocytes (25–30). Because simple diffusion of a compound is dependent on hydrophobic-hydrophilic properties, the reverse phase HPLC mobility of $7\beta\text{-NBD-NCT}$ was compared with that of cholytaurine (31–33). On a C-18 reverse phase column, using methanol–0.01 M sodium phosphate buffer, pH 7.5, 3:1 (v/v) as mobile phase, the retention time of 7.4 min for $7\beta\text{-NBD-NCT}$ was 2 min shorter than that determined for cholytaurine (not shown). This indicates qualitatively that $7\beta\text{-NBD-NCT}$ behaves in a slightly more hydrophilic manner than cholytaurine and, with regard to simple diffusion, no essential differences between the two bile salts should be expected.

In order to estimate the contribution of simple diffusion to total bile salt transport, uptake of $7\beta\text{-NBD-NCT}$ and of cholytaurine into freshly isolated hepatocytes was compared with their transport into hepatoma AS-30 D cells. In contrast to freshly isolated hepatocytes, the hepatoma cells exhibited no uptake of $7\beta\text{-NBD-NCT}$ during the time period required for determination of uptake velocity (Fig. 3A). Even at concentrations of up to 3 mM, no uptake of $7\beta\text{-NBD-NCT}$ into the hepatoma cells could be determined. Because, as with cholytaurine, no evidence for its uptake into hepatoma cells could be established and because other cell types as endothelial cells, adipocytes, and Hela cells exhibited the same behavior, the conclusion must be drawn that, under the experimental conditions used, transport of taurine-conjugated bile salts by simple diffusion does not have to be taken into account.

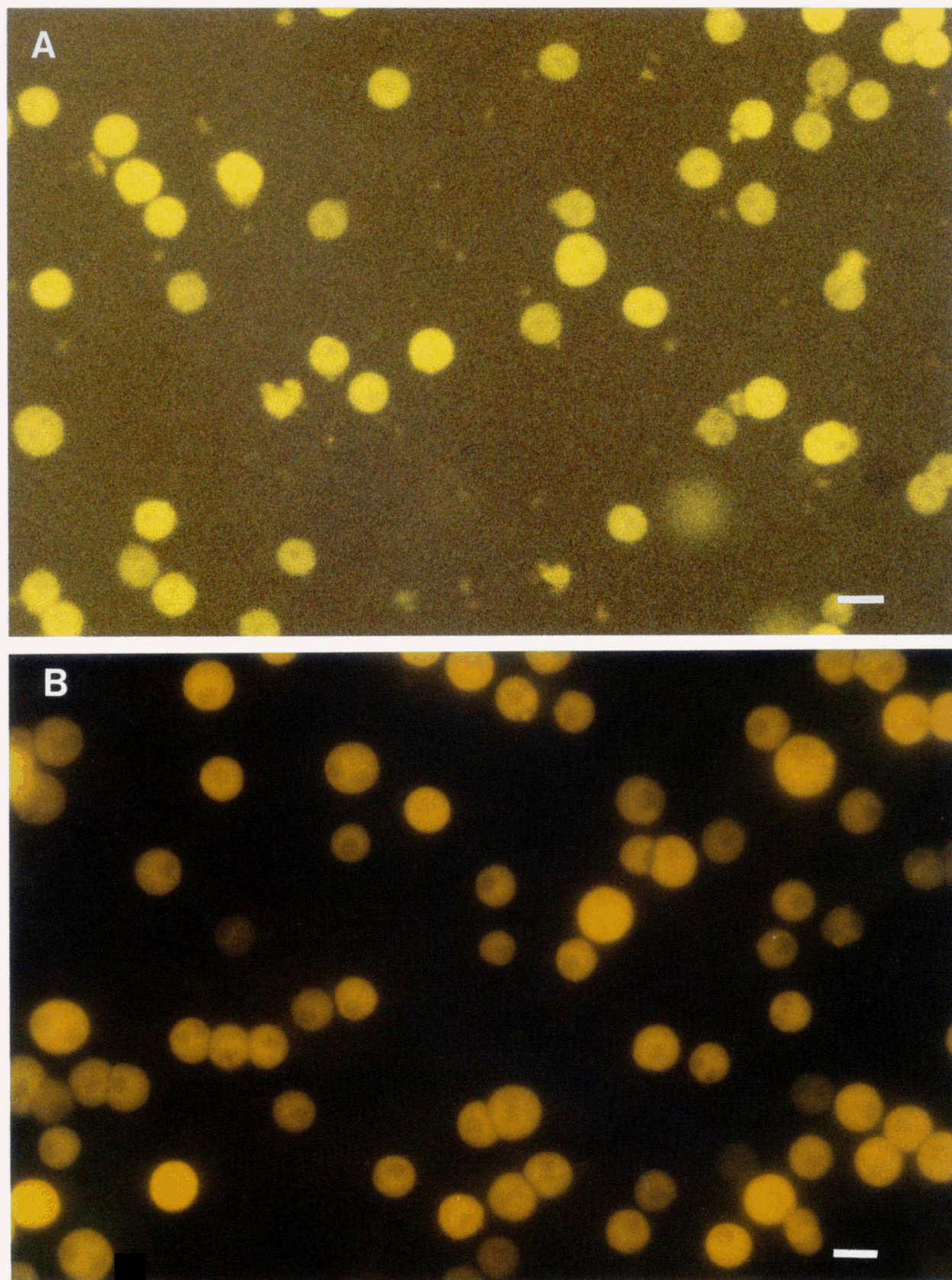


Fig. 2. Distribution of fluorescence after incubation of freshly isolated hepatocytes with 7β -NBD-NCT. A: Fluorescence micrograph after incubation of 1×10^6 freshly isolated hepatocytes with $5 \mu\text{M}$ 7β -NBD-NCT and 0.08% Trypan blue. Incubation time 45 sec (including exposure time). B: Fluorescence micrograph after incubation of the hepatocytes for 2 min. The cells were separated from the incubation medium by centrifugation and resuspended in standard buffer. Bar = $20 \mu\text{m}$.

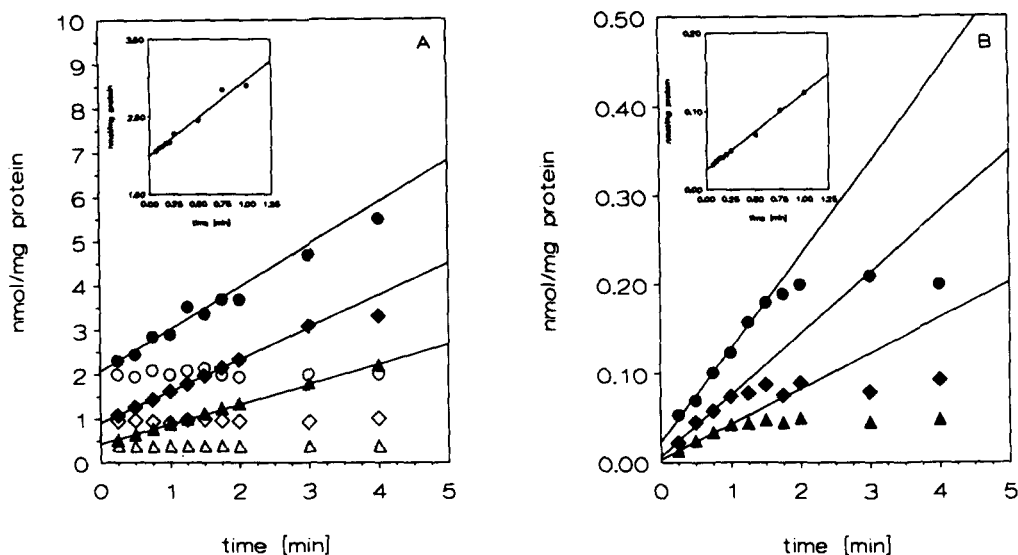


Fig. 3. Time-dependent uptake of 7β -NBD-NCT into freshly isolated hepatocytes (filled symbols) and hepatoma AS-30D cells (open symbols). Cells (1×10^6 – 2.5×10^6 cells/ml) were incubated with distinct concentrations of 7β -NBD-NCT each containing 37 kBq [^3H] 7β -NBD-NCT. A: Concentration of 7β -NBD-NCT: (\blacktriangle , \triangle) 100 μM , (\blacklozenge , \lozenge) 250 μM , (\bullet , \circ) 500 μM . Insert: Time scale from 0 to 60 sec. B: Concentration of 7β -NBD-NCT: (\blacktriangle) 1 μM , (\blacklozenge) 2 μM , (\bullet) 5 μM . Insert: Time scale from 0 to 60 sec.

Uptake of 7β -NBD-NCT into freshly isolated hepatocytes

The uptake of 7β -NBD-NCT into freshly isolated hepatocytes was determined in the concentration range from 1 μM to 1 mM. After a first concentration-dependent adsorption, influx was linear for about 1 to 2 min at higher concentrations (Fig. 3A) and for about 1 min at lower concentrations (Fig. 3B).

In order to ascertain that the linearity of uptake against time measured between 15 sec and 60 sec is not caused by intracellular trapping or by product accumulation, control experiments were performed in the time period before 15 sec. Initial linearities determined between 2 sec and 15 sec showed no significant differences when compared to the values obtained between 15 sec and 60 sec for either the high concentrations (Fig. 3A, insert) or for the low concentrations (Fig. 3B, insert). Because the uptake of the physiological bile salt cholytaurine into freshly isolated hepatocytes is strongly dependent on the concentration of extracellular Na^+ (19, 25, 27, 34–36), all uptake studies with 7β -NBD-NCT were performed in presence of a Na^+ concentration in the physiological range (143 mM) and in a medium depleted of Na^+ (1 mM). The dependency of initial influx rates on the extracellular concentration of 7β -NBD-NCT exhibited saturability, both in the presence of Na^+ and in the case of Na^+ depletion (Fig. 4A). It becomes apparent that, in comparison to the uptake of cholytaurine, transport of 7β -NBD-NCT exhibits only a small dependency on the presence of Na^+ . In order to analyze whether the saturation curves (Fig. 4A) follow the kinetic mechanism for a simple carrier-mediated transport or whether more complex mechanisms have to be

taken into account, the initial influx rates were plotted using the J/A -versus- J plot (Fig. 4B). This is the best plot to provide an indication that more than one simple transport system or site is involved. The graph exhibited a marked deviation from linearity, thus excluding that the uptake of 7β -NBD-NCT into isolated hepatocytes may be described by the equation for a simple transport process. Disregarding more complex mechanisms, the simplest kinetic assumption, two transport systems acting in parallel, was analyzed to examine its compatibility with the kinetic data. Total uptake of 7β -NBD-NCT then obeys the flux equation 1:

$$J = \frac{J_1 \cdot A}{K_{T1} + A} + \frac{J_2 \cdot A}{K_{T2} + A} \quad \text{Eq. 1)}$$

The symbols used are defined in Table 1.

In order to get approximate values of the kinetic parameters for 7β -NBD-NCT uptake, the J/A -versus- J plot was analyzed graphically and the values obtained were used as initial estimates for the calculation of the final kinetic parameters with the aid of the nonlinear least-squares regression analysis program ENZFITTER from the J -versus- A plot.

The kinetic parameters for the uptake of 7β -NBD-NCT into freshly isolated hepatocytes in presence of Na^+ , calculated from the means of the kinetic data obtained from 15 separate studies, are:

$$\begin{aligned} J_{1(\text{Na}^+143)} &= 0.15 \pm 0.03 \text{ nmol}/(\text{min} \cdot \text{mg protein}), \\ K_{T1(\text{Na}^+143)} &= 3.5 \pm 0.5 \mu\text{M}, \\ J_{2(\text{Na}^+143)} &= 1.00 \pm 0.10 \text{ nmol}/(\text{min} \cdot \text{mg protein}), \\ K_{T2(\text{Na}^+143)} &= 190 \pm 25 \mu\text{M}. \end{aligned}$$

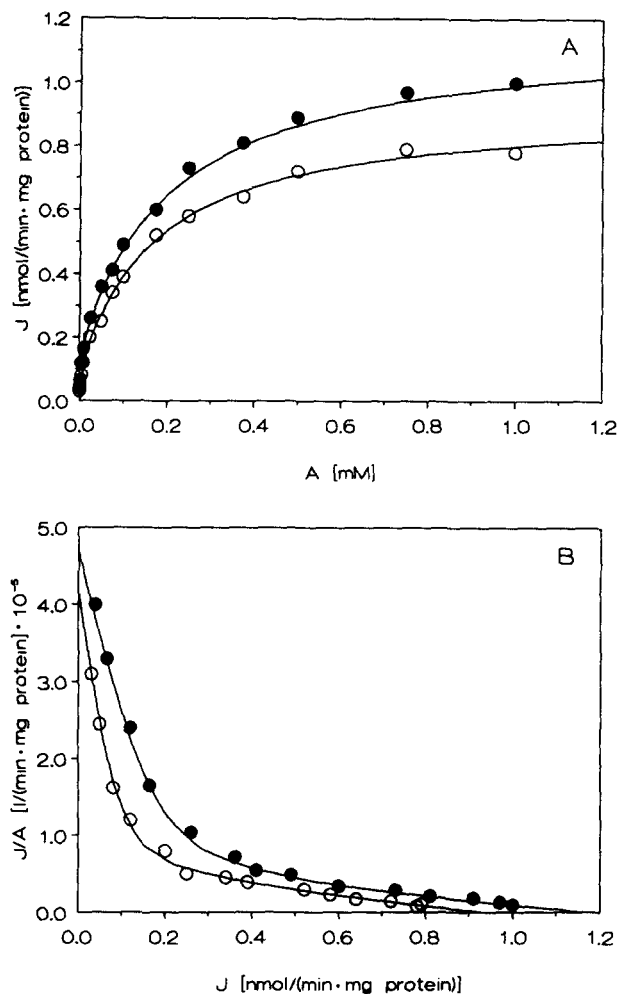


Fig. 4. Dependency of initial flux rates of 7β -NBD-NCT into isolated hepatocytes on 7β -NBD-NCT concentration; (●) in the presence of 143 mM Na^+ (standard buffer) and (○) in presence of 1 mM Na^+ (Na^+ -depleted medium). A: J-versus-A plot, B: J/A-versus-J plot. Curves were calculated applying equation 1.

The transport system with the lower maximal flux rate J_1 is characterized by a half-saturation constant K_{T1} which is about 50-fold lower than the half-saturation constant K_{T2} of the transport system with the higher maximal flux rate J_2 . The kinetic parameters calculated for the case of Na^+ depletion are:

$$\begin{aligned} J_{1(\text{Na}^+)} &= 0.10 \pm 0.03 \text{ nmol}/(\text{min} \cdot \text{mg protein}), \\ K_{T1(\text{Na}^+)} &= 3.0 \pm 0.05 \mu\text{M}, \\ J_{2(\text{Na}^+)} &= 0.85 \pm 0.09 \text{ nmol}/(\text{min} \cdot \text{mg protein}), \\ K_{T2(\text{Na}^+)} &= 195 \pm 27 \mu\text{M}. \end{aligned}$$

The dependencies of influx rates on concentration of 7β -NBD-NCT in the presence of Na^+ and with Na^+ -depletion, calculated from the kinetic parameters and provided with the experimentally determined error bars, are illustrated in **Fig. 5**. Albeit small, the degree of Na^+ dependency of uptake of 7β -NBD-NCT proved to be statistically significant ($P < 0.05$). The kinetic parameters demonstrate clearly that uptake of 7β -NBD-NCT shows a dependency on the presence of Na^+ for both transport systems. The maximal flux rates of J_1 and J_2 decreased to about 70% and 85%, respectively, as compared to the corresponding maximal flux rates in the presence of Na^+ . Whereas in case of Na^+ depletion the K_{T1} -value is slightly decreased, the K_{T2} -value remained practically unchanged.

Inhibition of 7β -NBD-NCT uptake by cholytaurine

The dependency of the initial flux rates on the concentration of 7β -NBD-NCT was studied in the presence of appropriate concentrations of cholytaurine. The inhibitory effect of cholytaurine on the initial flux rates of 7β -NBD-NCT in presence of Na^+ is shown in the J-versus-A plot (**Fig. 6A**). In order to show the type of this inhibition graphically the kinetic data were plotted in the J/A-versus-J plot (**Fig. 6B**). The different curves intersect the abscissa in one single point, demonstrating that the total maximal flux rate remained constant. Cholytaurine acts only to increase the apparent K_T -values, indicating that it behaves as a competitive inhibitor. With the well-based assumption that the presence of cholytaurine results in a competitive inhibition of uptake of 7β -NBD-NCT by both transport systems, the flux equation is:

$$J = \frac{J_1 \cdot A}{K_{T1}(1 + I/K'_{I1}) + A} + \frac{J_2 \cdot A}{K_{T2}(1 + I/K'_{I2}) + A} \quad \text{Eq. 2}$$

The symbols are defined in Table 1.

TABLE 1. List of symbols and definitions

Symbol	Definition	Unit
A	Concentration of substrate	mM
I	Concentration of inhibitor	mM
J	Flux rate	nmol/(min · mg protein)
J_1	Maximal flux rate of transport system 1	nmol/(min · mg protein)
J_2	Maximal flux rate of transport system 2	nmol/(min · mg protein)
K_T	Half-saturation constant of transport	μM
K_{T1}	Half-saturation constant of transport system 1	μM
K_{T2}	Half-saturation constant of transport system 2	μM
K_I	Inhibition constant of transport	μM
K_{I1}	Inhibition constant of transport system 1	μM
K_{I2}	Inhibition constant of transport system 2	μM

Subscripts added in parentheses give Na^+ concentration under the experimental conditions. For the competing substrate A' symbols are indicated by a prime.

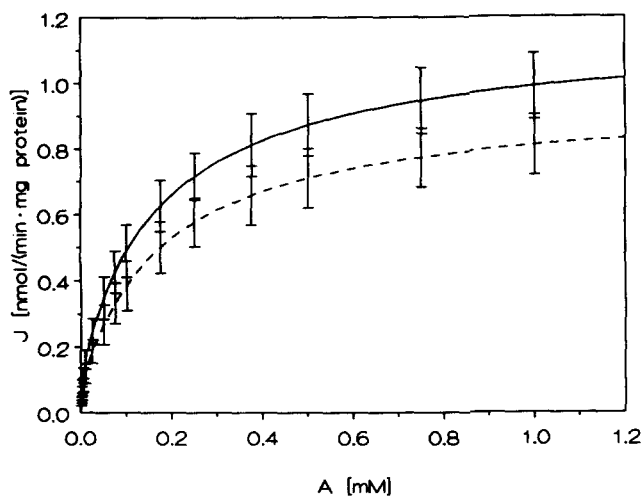


Fig. 5. Dependency of initial flux rates of 7β -NBD-NCT into isolated hepatocytes on 7β -NBD-NCT concentration; solid line, in presence of 143 mM Na^+ (standard buffer); dotted line, in presence of 1 mM Na^+ (Na^+ -depleted medium). The curves were calculated from the kinetic parameters obtained as the means \pm SEM of 15 determinations.

The experimental data were fitted to equation 2, using the kinetic parameters determined for the uptake of 7β -NBD-NCT as constant values and K'_I -values obtained by graphical analysis of the J/A -versus- A plot (Fig. 6B) as initial estimates. Regression analysis resulted in the inhibition constants K'_I for the inhibition of uptake of 7β -NBD-NCT in the presence of cholytaurine. In the presence of physiological concentrations of Na^+ , the K'_I -values for the two transport systems of 7β -NBD-NCT are:

$$K'_{I1(\text{Na}^+143)} = 17.5 \pm 2.1 \mu\text{M}$$

$$K'_{I2(\text{Na}^+143)} = 36.4 \pm 4.2 \mu\text{M}.$$

Because uptake of 7β -NBD-NCT and of cholytaurine exhibit a clearly different Na^+ dependency, the inhibition studies were likewise performed with Na^+ depletion (Figs. 7A and 7B). Even in the case of Na^+ depletion the competitive inhibition was evident. The two determined K'_I -values are:

$$K'_{I1(\text{Na}^+1)} = 8.5 \pm 1.0 \mu\text{M}$$

$$K'_{I2(\text{Na}^+1)} = 38.0 \pm 4.6 \mu\text{M}.$$

In presence of Na^+ the K'_I -values differ by a factor about 2, and with Na^+ depletion by a factor about 4.

If cholytaurine does not act as a classical competitive inhibitor but is a true competing substrate A' for both transport systems or sites, its K'_I -values are identical with its half-saturation constants K'_T and the flux equation 2 changes to equation 3:

$$J = \frac{J_1 \cdot A}{K_{T1}(1 + A'/K'_{T1}) + A} + \frac{J_2 \cdot A}{K_{T2}(1 + A'/K'_{T2}) + A} \quad \text{Eq. 3}$$

If cholytaurine is a substrate for only one of the two transport systems and for the other a competitive inhibi-

tor, combinations of one of the terms of flux equation 2 with the complementary term of flux equation 3 have to be considered. All possible cases are kinetically indistinguishable without further experimental evidence.

Uptake of cholytaurine into freshly isolated hepatocytes

Transport of cholytaurine was studied to clarify the mutual effects of 7β -NBD-NCT and cholytaurine on their uptake into freshly isolated hepatocytes with regard to the two transport systems deduced for transport of 7β -NBD-NCT. The dependency of initial influx rates on the concentration of cholytaurine, determined in the concentration range from 1 μM to 1 mM and shown in the J -versus- A plot, exhibited in the presence of Na^+ and with Na^+ depletion clear saturability (Fig. 8A). The J/A -versus- J

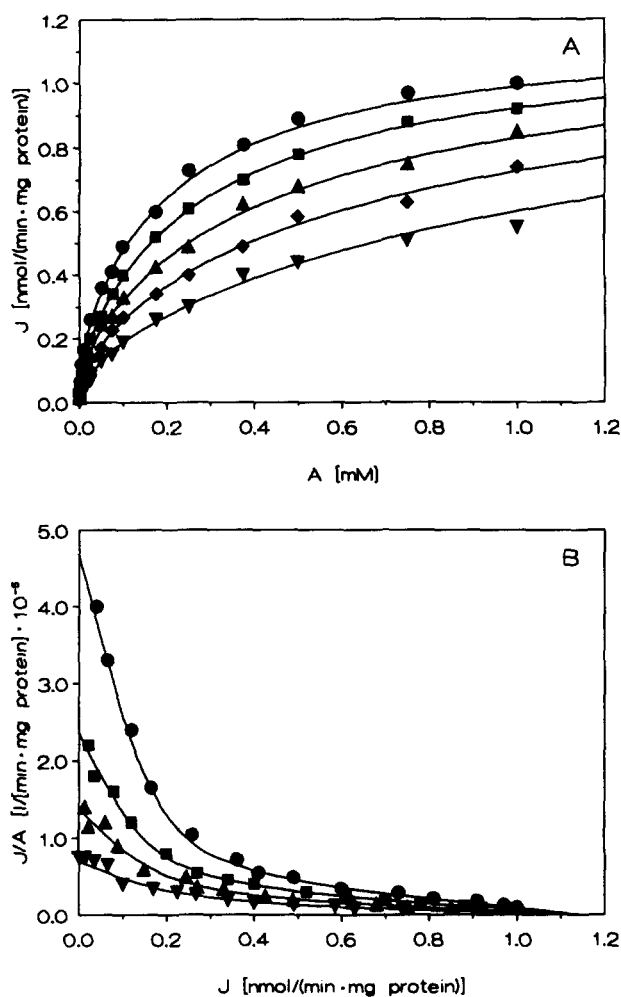


Fig. 6. Effect of different concentrations of cholytaurine on the dependency of initial flux rates of 7β -NBD-NCT into isolated hepatocytes on 7β -NBD-NCT concentration in presence of 143 mM Na^+ (standard buffer); (●) in absence of cholytaurine, and in presence of (■) 20 μM , (▲) 50 μM , (◆) 100 μM , (▼) 200 μM cholytaurine. A: J -versus- A plot, B: J/A -versus- J plot (for the sake of clarity, data in presence of 100 μM cholytaurine were not drawn). Curves were calculated applying equation 2.

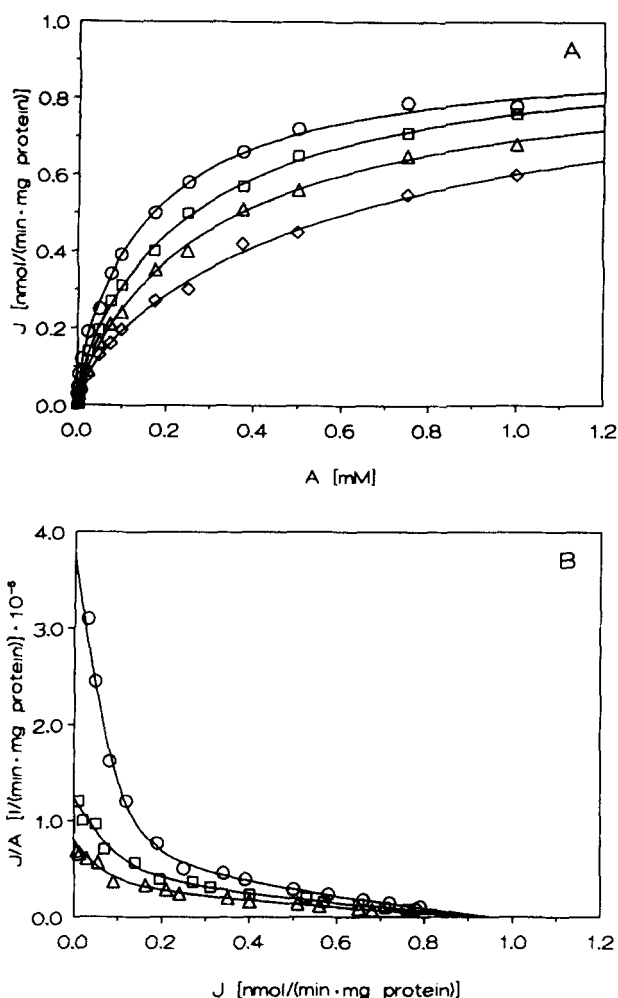


Fig. 7. Effect of different concentrations of cholytaurine on the dependency of initial flux rates of 7β -NBD-NCT into isolated hepatocytes on 7β -NBD-NCT concentration in presence of 1 mM Na^+ (Na^+ -depleted medium); (○) in absence of cholytaurine and in presence of (□) 20 μM , (△) 50 μM , (◇) 100 μM cholytaurine. A: J-versus-A plot, B: J/A-versus-J plot (for the sake of clarity, data in presence of 100 μM cholytaurine were not drawn). Curves were calculated applying equation 2.

plot demonstrates that the data obtained in the presence of Na^+ fit a curve that deviates only very slightly from linearity, whereas the curve fitting the data obtained with Na^+ -depletion exhibits a clear although small deviation from linearity (Fig. 8B). The significance of this deviation becomes evident by plotting the residual deviations against the flux rate after the experimental data in the J/A-versus-J plot have been fitted by linear regression (Fig. 9). The residual deviations show a lack of fit for a straight line (insert in Fig. 9) and have the signs to be expected for a concave downwards-shaped curve. This was obtained in all studies of cholytaurine uptake with Na^+ -depletion and demonstrates that, under these conditions, not one simple transport system for the uptake of cholytaurine into isolated hepatocytes is operative. The deviation from linearity in the J/A-versus-J plot is again compatible with the simplest assumption that two transport systems are acting in parallel and indicates that even

for the case of the presence of Na^+ a composite curve is obtained. However, in the J/A-versus-J plot the deviation from linearity for the experimental data obtained in the presence of Na^+ and even with Na^+ -depletion is so small that initial values based on linear transformation could not be estimated with the approximation necessary for a significant regression analysis (Fig. 8B). This being the case, the assumption was considered that 7β -NBD-NCT and cholytaurine are true competing substrates during uptake into hepatocytes. Consequently, the K'_I -values of the inhibition of uptake of 7β -NBD-NCT by cholytaurine should be identical with the K'_T -values for the uptake of cholytaurine. Therefore, these K'_I -values were used as K'_T -values for regression analysis of the experimental data and substituted in flux equation 1 for the determination of maximal flux rates for the uptake of cholytaurine by two transport systems acting in parallel. The kinetic parameters characterizing the two uptake sys-

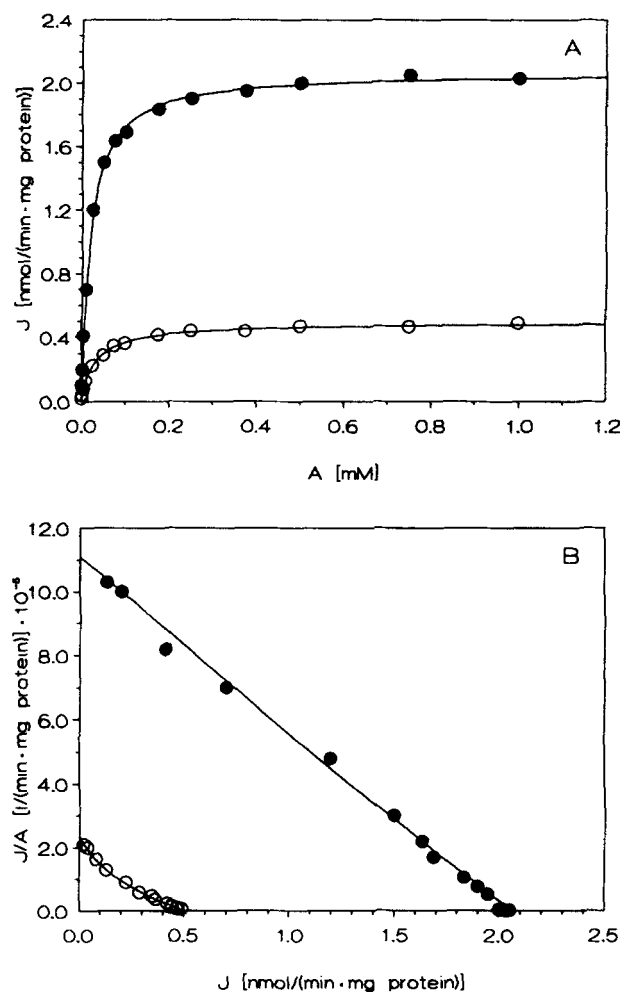


Fig. 8. Dependency of initial flux rates of cholytaurine into isolated hepatocytes on cholytaurine concentration; (●) in presence of 143 mM Na^+ (standard buffer) and (○) in presence of 1 mM Na^+ (Na^+ -depleted medium). A: J-versus-A plot, B: J/A-versus-J plot. Curves were calculated applying equation 1, using the K'_I -values of cholytaurine for the uptake of 7β -NBD-NCT.

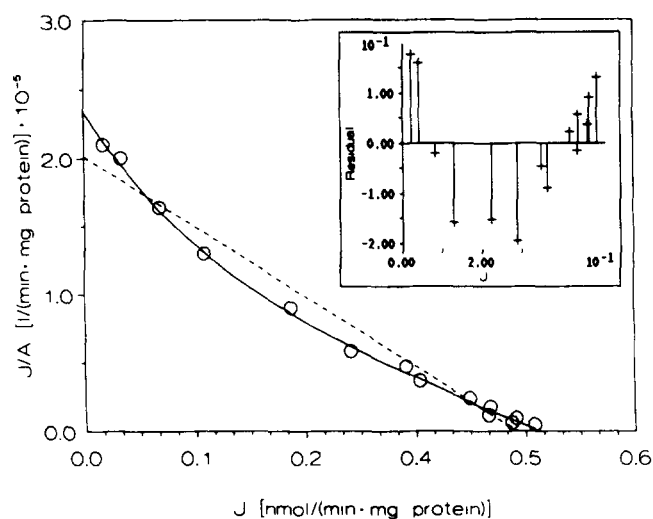


Fig. 9. Comparison of the fit of initial flux rates of cholytaurine, determined in presence of 1 mM Na⁺, in the J/A-versus-J plot to a straight line obtained by linear regression and to the curve applying equation 1. Insert: residual deviations versus flux rates for the straight line.

tems for cholytaurine in presence of Na⁺ are then:

$$\begin{aligned} J'_{1(\text{Na}^+143)} &= 1.55 \pm 0.14 \text{ nmol}/(\text{min} \cdot \text{mg protein}), \\ K'_{T1(\text{Na}^+143)} &= 16.1 \pm 3.0 \mu\text{M}, \\ J'_{2(\text{Na}^+143)} &= 0.51 \pm 0.05 \text{ nmol}/(\text{min} \cdot \text{mg protein}), \\ K'_{T2(\text{Na}^+143)} &= 38.0 \pm 4.1 \mu\text{M}, \end{aligned}$$

and for the uptake with Na⁺ depletion:

$$\begin{aligned} J'_{1(\text{Na}^+)} &= 0.10 \pm 0.02 \text{ nmol}/(\text{min} \cdot \text{mg protein}), \\ K'_{T1(\text{Na}^+)} &= 7.7 \pm 1.2 \mu\text{M}, \\ J'_{2(\text{Na}^+)} &= 0.40 \pm 0.03 \text{ nmol}/(\text{min} \cdot \text{mg protein}), \\ K'_{T2(\text{Na}^+)} &= 41.0 \pm 4.2 \mu\text{M}. \end{aligned}$$

The assumption of two transport systems, characterized by the above kinetic parameters, results in an excellent fit of the experimental data (Figs. 8A and 8B). Uptake of cholytaurine by both transport systems or sites exhibits a clear dependency on the presence of Na⁺. In case of Na⁺ depletion the maximal flux rate of transport system 1 decreased to about 10% as compared to the flux rate in presence of Na⁺. Maximal flux rate of transport system 2 decreased to about 80% with Na⁺ depletion.

Inhibition of cholytaurine uptake by 7β-NBD-NCT

In order to examine whether 7β-NBD-NCT competes with cholytaurine during uptake into hepatocytes and thus to justify the assumption that the two bile salts are competing substrates, the effect of the presence of 7β-NBD-NCT on the concentration dependency of the initial flux rates of cholytaurine was investigated. The presence of 7β-NBD-NCT exhibited a clear inhibitory effect on the uptake of cholytaurine in the presence of Na⁺ and with Na⁺ depletion, as shown in the J-versus-A plots (Fig. 10A and Fig. 11A). Graphical analysis in the J/A-versus-J diagrams (Figs. 10B and 11B) revealed a clear competitive in-

hibition not only in the presence of Na⁺ but also with Na⁺-depletion.

With the kinetic parameters derived for cholytaurine uptake, the inhibition constants of 7β-NBD-NCT for the uptake of cholytaurine were determined by regression analysis. For the uptake in presence of Na⁺ the K_I-values are:

$$\begin{aligned} K_{I1(\text{Na}^+143)} &= 4.5 \pm 1.1 \mu\text{M} \\ K_{I2(\text{Na}^+143)} &= 180 \pm 15 \mu\text{M}, \end{aligned}$$

and for the uptake with Na⁺ depletion:

$$\begin{aligned} K_{I1(\text{Na}^+)} &= 3.9 \pm 1.1 \mu\text{M} \\ K_{I2(\text{Na}^+)} &= 200 \pm 20 \mu\text{M}. \end{aligned}$$

The numerical values of the inhibition constants of 7β-NBD-NCT for the uptake of cholytaurine are in excellent agreement with the half-saturation constants determined for the uptake of 7β-NBD-NCT.

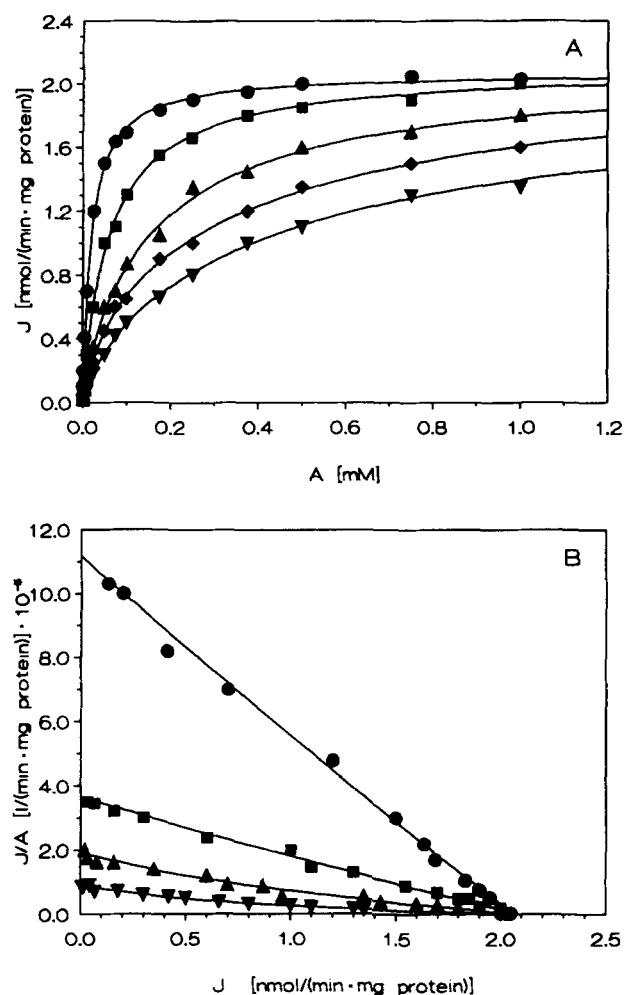


Fig. 10. Effect of different concentrations of 7β-NBD-NCT on the dependency of initial flux rates of cholytaurine into isolated hepatocytes on cholytaurine concentration in presence of 143 mM Na⁺ (standard buffer); (●) in absence of 7β-NBD-NCT, and in presence of (■) 10 μM, (▲) 50 μM, (◆) 100 μM, (▼) 200 μM 7β-NBD-NCT. A: J-versus-A plot, B: J/A-versus-J plot (for the sake of clarity, data in presence of 100 μM 7β-NBD-NCT were not drawn). Curves were calculated applying equation 2 using the kinetic parameters evaluated for uptake of cholytaurine.

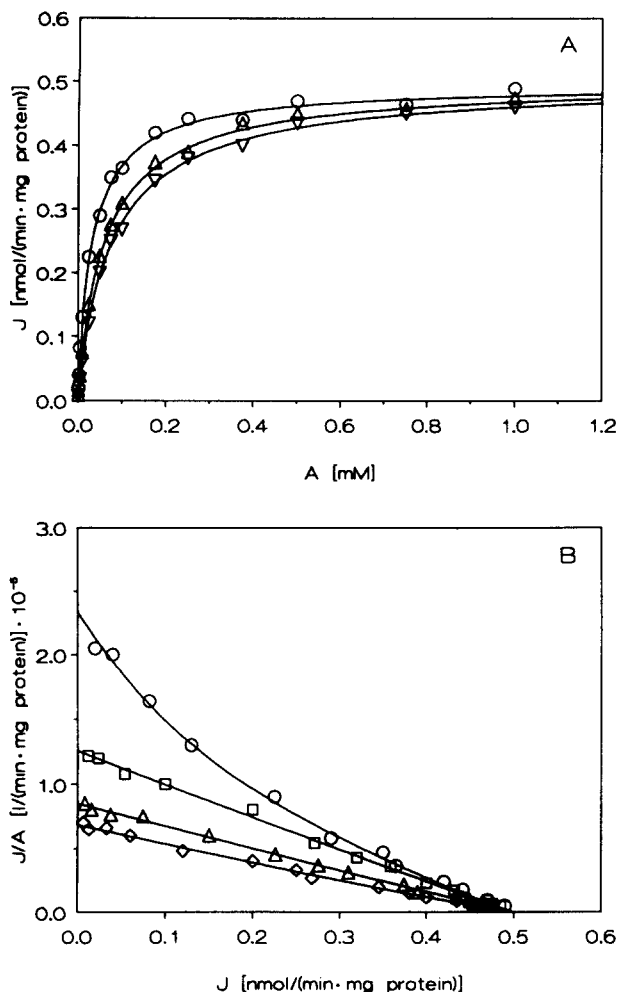


Fig. 11. Effect of different concentrations of 7β -NBD-NCT on the dependency of initial flux rates of cholytaurine into isolated hepatocytes on cholytaurine concentration in presence of 1 mM Na^+ (Na^+ -depleted medium); (○) in absence of 7β -NBD-NCT, and in presence of (□) 10 μM , (Δ) 50 μM , (\diamond) 100 μM 7β -NBD-NCT. A: J-versus-A plot (for the sake of clarity, data in presence of 10 μM 7β -NBD-NCT were not drawn), B: J/A-versus-J plot. Curves were calculated applying equation 2 using the kinetic parameters evaluated for uptake of cholytaurine.

Irreversible inhibition of bile salt uptake by photoaffinity labeling

The results obtained by the competition studies were confirmed by irreversible inhibition of both transport systems or sites by photoaffinity labeling using 7,7-ACT, a photolabile bile salt derivative that is taken up into freshly isolated hepatocytes within the error range with the same kinetic parameters as cholytaurine (G. Fricker and G. Kurz, unpublished results). In order to obtain a sufficiently high irreversible inhibition, photoaffinity labeling was performed with 400 μM 7,7-ACT. Subsequent to photoaffinity labeling, residual 7,7-ACT and its photolysis products were removed carefully to avoid a competitive inhibition of uptake of cholytaurine and 7β -NBD-NCT in addition to irreversible inhibition. Because of high experimental cost, these studies were performed in triplicate with each substrate only in the presence of Na^+ .

Irradiation of freshly isolated hepatocytes under the same experimental conditions in the absence of 7,7-ACT did not alter the uptake of 7β -NBD-NCT and cholytaurine. Photoaffinity labeling of freshly isolated hepatocytes resulted in the expected irreversible inhibition for the uptake of both 7β -NBD-NCT and cholytaurine, as shown by the decrease of the total maximal flux rate in the respective J-versus-A plots (Fig. 12).

With the approximate kinetic parameters for 7β -NBD-NCT uptake, obtained from the J/A-versus-J plot, regression analysis applying equation 1 resulted in the kinetic parameters:

$$J_{1(\text{Na}^{143})} = 0.09 \pm 0.03 \text{ nmol}/(\text{min} \cdot \text{mg protein}),$$

$$K_{T1(\text{Na}^{143})} = 4.0 \pm 0.5 \mu\text{M},$$

$$J_{2(\text{Na}^{143})} = 0.8 \pm 0.1 \text{ nmol}/(\text{min} \cdot \text{mg protein}),$$

$$K_{T2(\text{Na}^{143})} = 200 \pm 30 \mu\text{M}.$$

As to be expected for irreversible inhibition, the maximal flux rates are affected by photoaffinity labeling, whereas the half-saturation constants remained practically unaltered. Under the conditions used, the maximal flux rate of transport system 1 is decreased to about 60% and the maximal flux rate of transport system 2 is decreased to about 80%.

The effect of photoaffinity labeling of isolated hepatocytes on the uptake of cholytaurine was determined by regression analysis assuming that the K_T -values are not altered by photoaffinity labeling. This assumption has been shown to be valid for the uptake of 7β -NBD-NCT. By regression analysis the following flux rates were obtained:

$$J'_{1(\text{Na}^{143})} = 0.78 \pm 0.1 \text{ nmol}/(\text{min} \cdot \text{mg protein}),$$

$$J'_{2(\text{Na}^{143})} = 0.42 \pm 0.05 \text{ nmol}/(\text{min} \cdot \text{mg protein}).$$

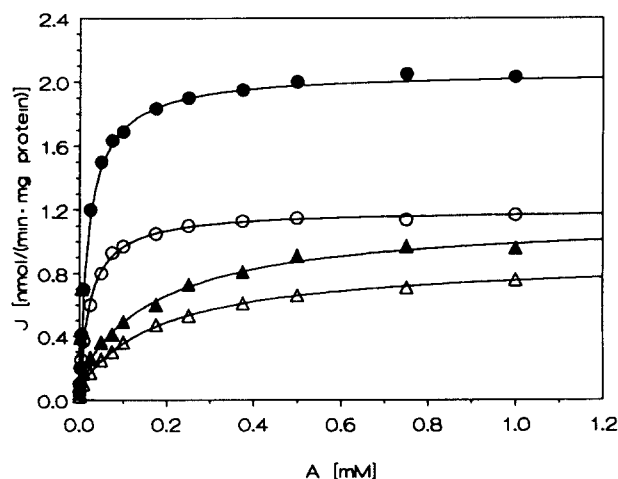


Fig. 12. Effect of photoaffinity labeling of isolated hepatocytes with 7,7-ACT on uptake of bile salts. Dependency of initial flux rates of cholytaurine into isolated hepatocytes on cholytaurine concentration in presence of 143 mM Na^+ (standard buffer); (●) no photoaffinity labeling and (○) after photoaffinity labeling. Dependency of initial flux rates of 7β -NBD-NCT into isolated hepatocytes on 7β -NBD-NCT concentration in presence of 143 mM Na^+ (standard buffer); (\blacktriangle) no photoaffinity labeling and (\triangle) after photoaffinity labeling. Curves were calculated applying equation 1.

The maximal flux rate of transport system 1 was decreased by photoaffinity labeling to about 55% and that of transport system 2 to about 80%.

For both bile salts, 7 β -NBD-NCT and cholytaurine, irreversible inhibition of their uptake into isolated hepatocytes by photoaffinity labeling affects the maximal flux rate of transport system 1 to the same extent, higher than that of transport system 2.

DISCUSSION

Hepatocytes in intact liver exhibit a morphological as well as a functional polarity; vectorial hepatobiliary transport of conjugated bile salts is achieved by different transport systems for uptake and secretion (16). Isolation of hepatocytes results, at least partially, in the loss of this polarity (37, 38). This loss of polarity does not exclude the fact that canalicular bile salt transport is still operational in isolated hepatocytes. Canalicular bile salt secretion has been demonstrated to be ATP-dependent (23, 24), but in the absence of the driving force this active process may occur as a facilitated transport mediated by the same transport system acting reversibly (21, 24, 39). This reversibility might have the effect that in addition to uptake by sinusoidal transport uptake by canalicular transport systems takes place. Before analyzing the kinetics of bile salt uptake it must be determined whether the true nature of the uptake studied with freshly isolated hepatocytes corresponds to sinusoidal uptake, to canalicular transport, or to both processes acting in parallel. Whereas by photoaffinity labeling no distinct bile salt binding polypeptide may be conclusively assigned to a specific sinusoidal uptake process, the canalicular membrane polypeptide with the apparent M_r of 110,000 will become photolabeled only if bile salt secretion is operative (16). This makes it possible to estimate the participation of the secretion system in bile salt uptake when freshly isolated hepatocytes are incubated with [^3H]ACT and subjected to photoaffinity labeling.

Photoaffinity labeling experiments using freshly isolated hepatocytes did not result in an incorporation of radioactivity in the bile salt-binding polypeptide with the apparent M_r of 110,000 (Fig. 1C), either during uptake of [^3H]ACT into the cells or during its efflux from preloaded cells. This contrasts with the photoaffinity labeling of membrane vesicles enriched with canalicular membranes and of intact liver tissue (Figs. 1A, 1B). In both systems, where the bile salt transport by the canalicular system has been detected (15, 16, 24), the canalicular membrane polypeptide became labeled.

With regard to the lack of photoaffinity labeling of the canalicular polypeptide with the apparent M_r 110,000, there is no indication that it may be due to proteolytic inactivation during collagenase perfusion. Furthermore, it

is probably not the result of a simple redistribution of the polypeptide with concomitant loss of polarity. The ability to interact with bile salts may be lost if the transport system is switched to a state not functionally active in bile salt transport or if different components of a complex transport system are separated by dissociation.

The photoaffinity labeling studies demonstrate that in freshly isolated hepatocytes the polypeptide involved in canalicular secretion is not accessible to photoaffinity labeling with photolabile bile salts. Because no bile salt transport across the lateral membrane of adherent cells has been observed so far with the fluorescent bile salt derivative (H-P. Buscher, H. Thom, U. Schramm, and G. Kurz, unpublished observations), the results indicate that freshly isolated hepatocytes have lost their capability for canalicular bile salt secretion and lead to the conclusion that the uptake of bile salts in isolated hepatocytes truly reflects only sinusoidal uptake. Consequently, it must be assumed that the efflux of conjugated bile salts from freshly isolated hepatocytes (40, 41) occurs by the reversal of their uptake.

Freshly isolated hepatocytes are heterogeneous with respect to uptake of 7 β -NBD-NCT (Fig. 2). The different capabilities of different hepatocytes for transport of bile salts may be conditioned by their localization in the acinus. In the intact liver acinus bile salt uptake into the hepatocytes is characterized by an acinar concentration gradient (1-3, 42-44). This acinar gradient, due to the decrease of the concentration of bile salts during their acinar passage, may be shaped by a gradient distribution of the relevant transport systems on the hepatocytes forming the acinus.

In order to get reproducible results, the heterogeneity of bile salt uptake of hepatocytes requires that the cell suspensions have reproducible composition. This is best guaranteed if the isolation procedure for hepatocytes comprises practically all the hepatocytes of the liver. Therefore, care has been taken that the isolation of hepatocytes was performed as completely and reproducibly as possible. With the isolation procedure described, it turned out that the strict observance of collagenase activities allowing the complete disintegration of a rat liver after 12-15 min of recirculating perfusion and a recovery phase for the isolated hepatocytes of 30-60 min leads to reproducible kinetic results.

Uptake of bile salts into hepatocytes is kinetically complex. Analysis of a complex system presupposes that one is fitting the kinetic data to the correct equation. In complex cases the discrimination between two models may often be kinetically impossible because the differences between them are in the range of experimental error. With the analysis of transport of conjugated bile salts a diffusion term is often subtracted from the determined flux rates without sufficient experimental justification (25-30). The subtraction of a diffusion term in a complex

system will predominantly affect systems that exhibit high half-saturation constants. In unfavorable cases the existence of an additional system characterized by a relative low activity and a relative high half-saturation constant may be completely suppressed.

Kinetic analysis of uptake of 7β -NBD-NCT and of cholytaurine studied up to 1 mM showed, by linear transformation in the J/A -versus- J plots (Figs. 4B and 8B), that no diffusion term must be taken into account. Because it is inconvenient to establish a small element of diffusion in cells having an effective mediated transport of taurine-conjugated bile salts such as hepatocytes, uptake of 7β -NBD-NCT and cholytaurine into hepatoma AS-30 D cells was studied. These cells, for which the absence of bile salt-binding membrane polypeptides has been demonstrated by photoaffinity labeling studies (45), were incubated with varying concentrations up to 3 mM of tritium-labeled 7β -NBD-NCT and cholytaurine, respectively. Uptake of both taurine-conjugated bile salts into the hepatoma cells could not be demonstrated during the multiple of time needed for an uptake determination, either for 7β -NBD-NCT or for cholytaurine. Furthermore, both taurine-conjugated bile salts do not cross the plasma membranes of other cell types having no transport systems for bile salts, so it must be assumed that compound lipid bilayers forming biological membranes are effective barriers for taurine-conjugated bile salts. Because no experimental evidence exists that taurine-conjugated bile salts could pass the lipid bilayer of a plasma membrane, there is no justification that an equation taking a diffusion term into account should be applied to uptake of taurine-conjugated bile salts into hepatocytes.

Uptake of 7β -NBD-NCT into freshly isolated hepatocytes in presence of Na^+ and with Na^+ -depletion occurs by saturable processes (Figs. 4A and 5). The analysis by linear transformation in the J/A -versus- J plot revealed, by the obvious deviation from linearity (Fig. 4B), that a simple transport system for the uptake of 7β -NBD-NCT is incompatible with the kinetic data. Disregarding more complex mechanisms, the shape of the curve may be described by different kinetic models based on different assumptions:

1. More than one simple transport system with different K_T -values;
2. One transport system with multiple sites with different K_T -values;
3. One transport system exhibiting negative cooperativity.

These different models cannot be distinguished by kinetic uptake studies with freshly isolated hepatocytes. Taking the dictum of formal logic "entia non sunt multiplicanda praeter necessitatem" (ascribed to William of Occam, c. 1280-1347) as a basis, the simplest kinetic model, as-

suming the existence of two different transport systems operating in parallel, was applied. This model is represented by equation 1 and the kinetic data were fitted to this equation in the J -versus- A plot using nonlinear regression. The excellent fit of the data shows, on the one hand, that no diffusion term has to be taken into account and justifies, on the other hand, the kinetic assumptions that were made. From analysis of the kinetic data it can be inferred that the uptake of 7β -NBD-NCT into freshly isolated hepatocytes is mediated in the presence of Na^+ as well as with Na^+ -depletion by two simple transport systems.

Uptake of 7β -NBD-NCT by both transport systems is competitively inhibited by the presence of cholytaurine (Figs. 6 and 7). Despite the fact that uptake of 7β -NBD-NCT and of cholytaurine exhibit a clear different dependency on the presence of Na^+ , competitive inhibition of both transport systems by cholytaurine was found not only in the presence of Na^+ (Fig. 6) but also in the case of Na^+ -depletion (Fig. 7).

In order to be useful as a true analogue of the physiological taurine-conjugated bile salts, 7β -NBD-NCT must share the same transport systems with them. Thus, hepatic uptake of cholytaurine was analyzed as to whether the same two transport systems deduced for the uptake of 7β -NBD-NCT are involved or not. Uptake of cholytaurine into freshly isolated hepatocytes occurs, as is expected (21, 27, 36) in the presence of Na^+ and with Na^+ -depletion by saturable processes (Fig. 8A). In a model comprising two distinct transport systems, one characterized by a higher K_T and a lower J_{max} value may easily evade detection. Therefore, as with 7β -NBD-NCT, the broad concentration range from 1 μM up to 1 mM has been selected for the initial rate studies with cholytaurine. Even using this broad concentration range, analysis of cholytaurine uptake by linear transformation resulted with the data obtained in the presence of Na^+ in the J/A -versus- J plot only in a slight and ambiguous deviation from linearity (Fig. 8B). However, with the data obtained with Na^+ -depletion, the deviation from linearity becomes unambiguously clear (Figs. 8B and 9). In consideration of the ratios of the K_T -values for the inhibition of 7β -NBD-NCT uptake obtained in the presence of Na^+ and with Na^+ -depletion, such behavior has to be expected if cholytaurine acts as a competing substrate for 7β -NBD-NCT uptake. These results show that with Na^+ -depletion a simple transport model for the uptake of cholytaurine is incompatible with the kinetic data and suggest that interpretation of the experimental data obtained with cholytaurine in the presence of Na^+ by a simple transport system does not satisfy the correct transport equation.

Because the initial estimates of the kinetic parameters for cholytaurine uptake obtainable from the linear transformation are subject to high errors, they could not be

used for fitting the data in the J-versus-A plot to equation 2 using nonlinear regression. Therefore, the applicability of equation 2 was examined by substitution of the K_T -values by the K_I -values, thereby lowering the number of parameters to be determined to the maximal flux rates. Identity of K_T - and K_I -values is required for competing substrates sharing the same transport system and has been demonstrated experimentally for the transport of amino acids (46, 47). The good fit (Fig. 8) to equation 2 demonstrates that the assumption of two distinct transport systems for sinusoidal uptake of cholytaurine both in the presence of Na^+ and with Na^+ -depletion is compatible with the kinetic data. Furthermore, the fit obtained by substitution of the K_T -values by the K_I -values of the inhibition of 7β -NBD-NCT uptake by cholytaurine also justifies the assumption that cholytaurine is transported by the same two transport systems involved in sinusoidal 7β -NBD-NCT uptake. This assumption is further strengthened by the inhibition of cholytaurine transport in the presence of 7β -NBD-NCT. A clear competitive inhibition of cholytaurine uptake into hepatocytes by two transport systems has been found in the presence of Na^+ and with Na^+ -depletion (Figs. 10B and 11B). The excellent agreement of the K_I -values for the inhibition of cholytaurine uptake with the K_T -values for the uptake of 7β -NBD-NCT (Table 2) justifies once more the assumption that cholytaurine is transported in the presence of Na^+ and with Na^+ -depletion into hepatocytes by two different transport systems.

The K_T -values of cholytaurine uptake in the presence of Na^+ , that is the K_I -values for the two transport systems mediating 7β -NBD-NCT uptake, being $K'_{T1} = 16.1 \pm$

$3.0 \mu\text{M}$ for transport system 1 and $K'_{T2} = 38.0 \pm 4.1 \mu\text{M}$ for transport system 2, differ only by a factor 2 (Table 2). The small difference in the K_T -values of the two transport systems makes their analysis by linearization ambiguous and by subtraction of a diffusion term the contribution of the higher K_T and lower maximal-flux-rate system will be suppressed, so that the duality of transport systems will be completely obscured. With Na^+ -depletion the K_T -values, i.e., K_I -values, differ by the factor 4 (Table 2) and the existence of two transport systems for cholytaurine uptake becomes more obvious.

The consistency of the kinetic data with a model comprising two sinusoidal transport systems for bile salts is clearly evidenced after irreversible inhibition of bile salt transport by photoaffinity labeling of freshly isolated hepatocytes (Fig. 12). Without affecting the K_T -values, the maximal flux rates were decreased in like manner for 7β -NBD-NCT as well as for cholytaurine.


7β -NBD-NCT and cholytaurine are both taurine-conjugated bile salts. From the analyses of the kinetic data of their uptake into freshly isolated hepatocytes it is inferred that they are competing substrates, whose sinusoidal transport is mediated by two distinct transport systems, both dependent on the presence of Na^+ . The dependency on the presence of Na^+ is, on the one hand, different for the two transport systems and, on the other hand, different for the two competing substrates. Differences in maximal flux rates, in K_T -values, and in dependencies on the influence of ions such as Na^+ are easy to imagine for structurally differing substrates. It may be sufficient for changing all kinetic data and dependencies that, in a multistep mechanism, the rate-determining step for different sub-

TABLE 2. Kinetic parameters of uptake of 7β -NBD-NCT and cholytaurine into freshly isolated hepatocytes

	Transport System 1			Transport System 2		
	K_{T1}	J_1	K'_{I1}	K_{T2}	J_2	K'_{I2}
7β -NBD-NCT	μM	$\text{nmol}/(\text{min} \cdot \text{mg protein})$	μM	μM	$\text{nmol}/(\text{min} \cdot \text{mg protein})$	μM
143 mM Na^+	3.5 ± 0.5	0.15 ± 0.03		190 ± 25	1.0 ± 0.1	
1 mM Na^+	3.0 ± 0.5	0.10 ± 0.03		195 ± 27	0.85 ± 0.09	
+ Cholytaurine, 143 mM Na^+			17.5 ± 2.1			36.4 ± 4.2
+ Cholytaurine, 1 mM Na^+			8.5 ± 1.0			38.0 ± 4.6
After photoaffinity-labeling, 143 mM Na^+	4.0 ± 0.5	0.09 ± 0.03		200 ± 30	0.8 ± 0.1	
Cholytaurine	K'_{T1}	J'_1	K_{I1}	K'_{T2}	J'_2	K_{I2}
	μM	$\text{nmol}/(\text{min} \cdot \text{mg protein})$	μM	μM	$\text{nmol}/(\text{min} \cdot \text{mg protein})$	μM
143 mM Na^+	16.1 ± 3.0	1.55 ± 0.14		38.0 ± 4.1	0.51 ± 0.05	
1 mM Na^+	7.7 ± 1.2	0.1 ± 0.02		41 ± 4.2	0.4 ± 0.03	
+ 7β -NBD-NCT, 143 mM Na^+			4.5 ± 1.1			180 ± 15
+ 7β -NBD-NCT, 1 mM Na^+			3.9 ± 1.1			200 ± 20
After photoaffinity-labeling, 143 mM Na^+	17.0 ± 3	0.78 ± 0.1		40 ± 4.5	0.42 ± 0.05	

strates is shifted from one to another individual step in the same transport system. The introduction of a relatively bulky substituent in the 7β -position of a taurine-conjugated bile salt may cause such a shifting. Because the hydrophobicities of 7β -NBD-NCT and cholyltaurine are not very different, the differences in the kinetic data of the two bile salts may be due to steric reasons.

The deduced kinetic model for sinusoidal uptake of taurine-conjugated bile salts is the simplest one describing all experimental results and has its justification for this reason. The proposed model does not provide information on the localization of the inferred two transport systems, which could either be operating in parallel in the same hepatocytes or represent two populations of hepatocytes. Whereas other models of comparable or higher complexity cannot be excluded, the applicability of an equation for a simple hyperbola has been disproven, and it has been shown that the analysis of a Na^+ -dependent bile salt transport by subtraction of flux rates obtained in the presence and in the absence of Na^+ is not justified kinetically. The final decision for the proposed model will be facilitated by nonkinetic methods and has come within easy reach now, with the first transporter for bile salts having been cloned (48, 49).

Independent of the detailed mechanisms of bile salt transport, 7β -NBD-NCT has been shown to be, in all respects, a competing substrate for hepatobiliary cholyltaurine transport not only in sinusoidal uptake but also in intracellular interactions and in canalicular secretion (5). Thus, it may be used for visualization of bile salt transport by fluorescence microscopy and to disclose the functional state of bile salt transport under physiological and pathophysiological conditions. Due to the favorable kinetic parameters of 7β -NBD-NCT for sinusoidal uptake and the small dependency on the presence of Na^+ , it is appropriate for elucidation of the acinar heterogeneity of sinusoidal transport systems for bile salts (50). 

This investigation was supported by the Deutsche Forschungsgemeinschaft and the Fritz-Thyssen-Stiftung. One of us (U. Schramm) is indebted to the Boehringer-Ingelheim-Fonds for a scholarship.

Manuscript received 9 March 1992 and in revised form 20 October 1992.

REFERENCES

1. Buscher, H-P., W. Gerok, G. Kurz, and S. Schneider. 1985. Visualization of bile salt transport with fluorescent derivatives. In *Enterohepatic Circulation of Bile Acids and Sterol Metabolism*. G. Paumgartner, A. Stiehl and W. Gerok, editors. MTP Press, Lancaster, England. 243-247.
2. Buscher, H-P., G. Fricker, W. Gerok, G. Kurz, M. Müller, S. Schneider, U. Schramm, and A. Schreyer. 1987. Hepatic transport systems for bile salts: localization and specificity. In *Bile Acids and the Liver with an Update on Gallstone Disease*. G. Paumgartner, A. Stiehl and W. Gerok, editors. MTP Press, Lancaster, England. 95-110.
3. Buscher, H-P., W. Gerok, M. Köllinger, G. Kurz, M. Müller, A. Nolte, and S. Schneider. 1988. Transport systems for amphipathic compounds in normal and neoplastic hepatocytes. *Adv. Enzyme Regul.* **27**: 173-192.
4. Schneider, S., U. Schramm, A. Schreyer, H-P. Buscher, W. Gerok, and G. Kurz. 1991. Fluorescent derivatives of bile salts. I. Syntheses and properties of NBD-amino derivatives of bile salts. *J. Lipid Res.* **32**: 1755-1767.
5. Schramm, U., A. Dietrich, S. Schneider, H-P. Buscher, W. Gerok, and G. Kurz. 1991. Fluorescent derivatives of bile salts. II. Suitability of NBD-amino derivatives of bile salts for the study of biological transport. *J. Lipid Res.* **32**: 1769-1779.
6. Kramer, W., and G. Kurz. 1983. Photolabile derivatives of bile salts. Synthesis and suitability for photoaffinity labeling. *J. Lipid Res.* **24**: 910-923.
7. Hübscher, G., G. R. West, and D. Brindley. 1965. Studies on the fractionation of mucosal homogenates from the small intestine. *Biochem. J.* **97**: 629-642.
8. Horder, M., and R. Rej. 1983. Alanine aminotransferase. In *Methods of Enzymatic Analysis*. 3rd ed. Vol III. H. U. Bergmeyer, editor. Verlag Chemie, Weinheim, Germany. 444-450.
9. Gebhardt, R., and G. Williams. 1986. Amino acid transport in established adult rat liver epithelial cell lines. *Cell Biol. Toxicol.* **2**: 9-20.
10. Trautschold, I., W. Lamprecht, and G. Schweitzer. 1985. UV-method with hexokinase and glucose-6-phosphate dehydrogenase. In *Methods of Enzymatic Analysis*. 3rd ed. Vol VII. H. U. Bergmeyer, editor. Verlag Chemie, Weinheim, Germany. 346-357.
11. Berry, M. N., and D. S. Friend. 1969. High-yield preparation of isolated rat liver parenchymal cells. A biochemical and fine structural study. *J. Cell. Biol.* **43**: 506-520.
12. Seglen, P. O. 1976. Preparation of isolated rat liver cells. *Methods Cell. Biol.* **13**: 29-83.
13. Berry, M. N., A. M. Edwards, G. J. Barritt, M. B. Grivell, H. J. Halls, B. J. Gannon, and D. S. Friend. 1991. Isolated hepatocytes. Preparation, properties and applications. In *Laboratory Techniques in Biochemistry and Molecular Biology*. Vol. 21. R. H. Burdon and P. H. van Knippenberg, editors. Elsevier, Amsterdam, New York, Oxford.
14. Page, R. A., K. M. Stowell, M. J. Hardman, and K. E. Kitson. 1992. The assessment of viability in isolated rat hepatocytes. *Anal. Biochem.* **200**: 171-175.
15. Ruetz, S., G. Fricker, G. Hugentobler, K. Winterhalter, G. Kurz, and P. J. Meier. 1987. Isolation and characterization of the putative canalicular bile salt transport system of rat liver. *J. Biol. Chem.* **262**: 11324-11330.
16. Fricker, G., S. Schneider, W. Gerok, and G. Kurz. 1987. Identification of different transport systems for bile salts in sinusoidal and canalicular membranes of hepatocytes. *Biol. Chem. Hoppe-Seyler* **368**: 1143-1150.
17. Laemmli, U. K. 1970. Cleavage of structural proteins during the assembly of the head of bacteriophage T4. *Nature*. **227**: 680-685.
18. Klingenberg, M., and E. Pfaff. 1967. Means of terminating reactions. *Methods Enzymol.* **10**: 680-684.
19. Schwarz, L. R., R. Burr, M. Schwenk, E. Pfaff, and H. Greim. 1975. Uptake of taurocholic acid into isolated rat liver cells. *Eur. J. Biochem.* **55**: 617-623.
20. Falk, E., M. Müller, M. Huber, D. Keppler, and G. Kurz. 1989. Direct photoaffinity labeling of leukotriene binding sites. *Eur. J. Biochem.* **186**: 741-747.
21. Ruetz, S., G. Hugentobler, and P. J. Meier. 1988. Functional reconstitution of canalicular bile salt transport sys-

- tem of rat liver. *Proc. Natl. Acad. Sci. USA*. **85**: 6147-6157.
22. Sippel, C. A., A. Ananthanarayanan, and F. S. Suchy. 1990. Isolation and characterization of the canalicular membrane bile acid transport protein of rat liver. *Am. J. Physiol.* **258**: G728-G737.
 23. Nishida, T., Z. Gatmaitan, M. Che, and J. M. Arias. 1991. Rat liver canalicular membrane vesicles contain ATP-dependent bile acid transport system. *Proc. Natl. Acad. Sci. USA*. **88**: 6590-6594.
 24. Müller, M., T. Ishikawa, U. Berger, C. Klünemann, L. Lucka, A. Schreyer, C. Kannicht, W. Reutter, G. Kurz, and D. Keppler. 1991. ATP-dependent transport of taurocholate across the hepatocyte canalicular membrane mediated by a 110-kDa glycoprotein binding ATP and bile salt. *J. Biol. Chem.* **266**: 18920-18926.
 25. Anwer, M. S., and D. Hegner. 1978. Effect of Na⁺ on bile acid uptake by isolated hepatocytes. Evidence for a heterogeneous system. *Biol. Chem. Hoppe-Seyler*. **359**: 181-192.
 26. Iga, T., and C. D. Klaassen. 1982. Uptake of bile acids by rat hepatocytes. *Biochem. Pharmacol.* **31**: 211-216.
 27. Hardison, W. G. M., S. Bellentani, V. Heasley, and D. Shellhamer. 1984. Specificity of an Na⁺-dependent taurocholate transport site in isolated hepatocytes. *Am. J. Physiol.* **246**: G477-G483.
 28. Hardison, W. G. M., P. J. Lowe, and E. Gosink. 1988. Nature of taurodehydrocholic acid uptake in rat hepatocytes. *Am. J. Physiol.* **254**: G269-G274.
 29. Kukongviriyapan, V., and N. H. Stacey. 1989. Comparison of uptake kinetics in freshly isolated suspensions and short-term primary cultures of rat hepatocytes. *J. Cell. Physiol.* **140**: 491-497.
 30. Hardison, W. G. M., V. L. Heasley, and D. F. Shellhamer. 1991. Specificity of the hepatocyte Na⁺-dependent taurocholate transporter: influence of side chain length and charge. *Hepatology*. **13**: 68-72.
 31. Armstrong, M. J., and M. C. Carey. 1982. The hydrophobic-hydrophilic balance of bile salts. Inverse correlation between reverse-phase high performance liquid chromatographic mobilities and micellar cholesterol-solubilizing capacities. *J. Lipid Res.* **23**: 70-80.
 32. Heuman, D. M. 1989. Quantitative estimation of the hydrophilic-hydrophobic balance of mixed bile salt solutions. *J. Lipid Res.* **30**: 719-730.
 33. Roda, A., A. Minutello, M. A. Angellotti, and A. Fini. 1990. Bile acid structure-activity relationship: evaluation of bile acid lipophilicity using 1-octanol/water partition coefficient and reverse phase HPLC. *J. Lipid Res.* **31**: 1433-1443.
 34. Minder, E., and G. Paumgartner. 1979. Disparate Na⁺-requirement of taurocholate and indocyanine green uptake by isolated hepatocytes. *Experientia*. **35**: 888-890.
 35. Blitzer, B. L., S. L. Ratoosh, C. B. Donovan, and J. L. Boyer. 1982. Effects of inhibitors of Na⁺-coupled ion transport on bile acid uptake by isolated hepatocytes. *Am. J. Physiol.* **243**: G4-G53.
 36. Anwer, M. S., A. U. Branson, and J. M. Atkinson. 1991. Mechanism of inhibition of hepatic bile acid uptake by amiloride and 4,4'-diisothiocyano-2,2'-disulfonic stilbene (DIDS). *Biochem. Pharmacol.* **42**: 135-141.
 37. Groothuis, G. M. M., C. E. Hulstaert, D. Kalicharan, and M. J. Hardonk. 1981. Plasma membrane specialization and intracellular polarity of freshly isolated rat hepatocytes. *Eur. J. Cell Biol.* **26**: 43-51.
 38. Nickola, I., and M. Frimmer. 1986. Preservation of cellular polarity in isolated hepatocytes. *Cell Tissue Res.* **243**: 437-440.
 39. Garrahan, P. J., and I. M. Glynn. 1967. The sensitivity of the sodium pump to external sodium. *J. Physiol.* **192**: 175-188.
 40. Anwer, M. S., R. Kroker, and D. Hegner. 1975. Bile acids secretion and synthesis by isolated rat hepatocytes. *Biochem. Biophys. Res. Commun.* **64**: 603-609.
 41. Schwarz, L. R., M. Schwenk, E. Pfaff, and H. Greim. 1976. Excretion of taurocholate from isolated hepatocytes. *Eur. J. Biochem.* **71**: 369-373.
 42. Jones, A. L., G. T. Hradek, R. H. Renston, K. Y. Wong, G. Karlaganis, and G. Paumgartner. 1980. Autoradiographic evidence for hepatic lobular concentration gradient of bile acid derivative. *Am. J. Physiol.* **238**: G233-G237.
 43. Groothuis, G. M. M., M. J. Hardonk, K. P. T. Keulemans, P. Nieuwenhues, and D. K. F. Meijer. 1982. Autoradiographic and kinetic demonstration of acinar heterogeneity of taurocholate transport. *Am. J. Physiol.* **243**: G455-G462.
 44. Buscher, H-P., U. Schramm, S. MacNelly, G. Kurz, and W. Gerok. 1991. The acinar location of the sodium-independent and the sodium-dependent component of taurocholate uptake. A histoautoradiographic study of rat liver. *J. Hepatol.* **13**: 169-179.
 45. Kröncke, K. D., G. Fricker, P. J. Meier, W. Gerok, T. Wieland, and G. Kurz. 1986. α -Amanitin uptake into hepatocytes. Identification of hepatic membrane transport systems used by amatoxins. *J. Biol. Chem.* **261**: 12562-12567.
 46. Christensen, H. N., M. Liang, and E. G. Archer. 1967. A distinct Na⁺-requiring transport system for alanine, serine, cysteine, and similar amino acids. *J. Biol. Chem.* **242**: 5237-5246.
 47. Christensen, H. N. 1969. Some special kinetic problems of transport. *Adv. Enzymol.* **32**: 1-20.
 48. Hagenbuch, B., H. Lübbert, B. Stieger, and P. J. Meier. 1990. Expression of the hepatocyte Na⁺/bile acid cotransporter of *Xenopus laevis* oocytes. *J. Biol. Chem.* **265**: 5357-5360.
 49. Hagenbuch, B., B. Stieger, M. Fouget, H. Lübbert, and P. J. Meier. 1991. Functional expression cloning and characterization of the hepatocyte Na⁺/bile acid cotransport system. *Proc. Natl. Acad. Sci. USA*. **88**: 10629-10633.
 50. Buscher, H-P., G. Fricker, W. Gerok, G. Kurz, and U. Schramm. 1993. The sinusoidal transport system for taurine-conjugated bile salts. In *Bile Acids and the Hepatobiliary System*. G. Paumgartner, A. Stiehl, and W. Gerok, editors. Kluwer Academic Publishers, Dordrecht, The Netherlands. 105-117.